Carrier dynamics and intraminiband coupling in semiconductor superlattices

C. P. Holfeld,[1] W. Schäfer,[2] and K. Leo[1]
[1]*Institut für Angewandte Photophysik, Technische Universität Dresden, 01062 Dresden, Germany*
[2]*Institut für Schichten und Grenzflächen, Forschungszentrum Jülich, 52425 Jülich, Germany*
(Received 30 May 2003; published 26 September 2003)

The Coulomb coupling between Wannier-Stark excitons and the continuum of lower-lying states in an electrically biased superlattice leads not only to pronounced Fano resonances, but has also a heavy impact on the nonlinear polarization dynamics. The strong variation of line broadening in linear spectra with the electric field, however, is not reflected in the dephasing rate. Moreover, increasing the excitation density leads to a linear growth of the time-resolved four-wave-mixing signal instead of a cubic dependence. We present a theory based upon the Born-Markov equations of a superlattice. The unusual polarization dynamics can be traced back to the interference resulting from the simultaneous occupation of different Wannier-Stark subbands and the relaxation of these nonequilibrium distributions.

DOI: 10.1103/PhysRevB.68.125325 PACS number(s): 71.35.Gg, 42.50.Md, 71.35.Cc, 78.67.Pt

The Fano coupling of quantum-mechanical states is a widespread phenomenon found in a large variety of natural and artificial systems. Such coupling occurs whenever a discrete state interacts with a degenerate continuum, with both being excited from a common ground state. In the linear response, the Fano interaction is reflected by a characteristic asymmetric line broadening in conjunction with a dip below the former continuum level. Since the degeneracy of a discrete state and continuum is a fundamental situation, Fano resonances have been identified in virtually all physical areas. These include, for instance, different effects such as Auger ionization in atoms,[1] molecular dissociation of hydrogen,[2] conductance of a single-electron transistor,[3] or acoustic transmission in sonic crystals.[4] While the Fano coupling is observed in the frequency domain in most cases, the impact of the broadening on the dynamics remains unclear.

Particularly, the Fano effect exists generally in low-dimensional semiconductors due to Coulomb interaction of confined subbands. Compared to the linear response, manifestations of Fano interferences in nonlinear spectroscopy[5] and transport[3] occur in a much richer diversity for at least two reasons: The interference effects depend on the coherent and incoherent occupation of bound and continuum states and the coupling of the states additionally effects scattering and dephasing processes. Theoretical investigations of these interference effects have been restricted to models in which relaxation processes are treated by phenomenological dephasing rates.[6,7]

Here we report on the influence of Fano coupling on dephasing and relaxation processes in semiconductor superlattices. In an electric field, these structures exhibit a regular ladder of energy states with a field-dependent separation (Wannier-Stark ladder). Because of their excitonic nature, every ladder step consists of discrete bound states below an ionization continuum of unbound states. The Fano effect occurs due to coupling of such discrete Wannier-Stark excitons to the continua of lower ladder states. As a unique feature of superlattices, the Fano coupling strength can be directly accessed in experiment: It can be varied by tuning the electric bias field. A growing separation of the Wannier-Stark subbands within the same miniband increases the momentum mismatch and decreases overlap of the states hence reducing their mutual interaction. In linear spectroscopy the Fano interaction is directly apparent in the typical line shape of the coupled transitions[8] but the dynamics of the resonance remains to be explored.

In this paper, we focus on the carrier and polarization dynamics in the nonlinear regime where a mixing of Wannier-Stark states and a simultaneous occupation of different subbands has not yet been considered. Already simplified models show that the Fano broadening of linear spectra does not transform into a faster single exponential decay of time-resolved four-wave-mixing (TR FWM) signals. For a single bound state resonant with a continuum, the interference of the corresponding transitions results in a single dip in the signal. This dip decreases when the ratio of bound state and continuum oscillator strength is increased.[6] We find that this destructive interference effect dominates the TR FWM signals over several orders of magnitude. In addition, the intraminiband coupling results in a fast decay of the occupation modulation in a FWM experiment, which in turn is strongly manifested in an unusual density dependence of the TR FWM signal intensity.

For the experiments we have used high-quality $GaAs/Al_{0.3}Ga_{0.7}As$ superlattices with 35 periods of 67 Å and 17 Å wide well and barrier, respectively, corresponding to a miniband width of 35 meV. A homogeneous electric field is applied along the growth direction via an Ohmic contact on the substrate and a semitransparent Schottky contact on the superlattice side. The separation of the Wannier-Stark ladder is then varied by this bias field. Since we use a transmission geometry for our experiments, the opaque substrate is partially removed in a wet-etching process.

This system is theoretically modeled as follows. The one-particle eigenstates of the superlattice with energies $E_n^{c,v}(\mathbf{k})$, are represented in the usual envelope-function approximation as

$$\psi_n^{c,v}(\mathbf{k},\mathbf{r}) = \frac{1}{\sqrt{A}} \exp(i\mathbf{k}\cdot\boldsymbol{\rho})\,\phi_n^{c,v}(z)\,u_0^{c,v}(\mathbf{r}), \qquad (1)$$

where the plane-wave states depend on the in-plane vector $\boldsymbol{\rho}$ and the parallel wave vector $\mathbf{k}$. $u_0^{c,v}(\mathbf{r})$ are the lattice-periodic functions of the barrier and well materials at the Γ point, and the Wannier-Stark states $\phi_n^{c,v}(z)$ are eigenstates of the effective-mass Hamiltonian

$$h^{c,v}(z) = -\frac{\hbar^2}{2m^{c,v}(z)}\frac{\partial^2}{\partial z^2} - eFz + U_{c,v}(z). \tag{2}$$

We assume an extended system, for which $U_{c,v}(z)$ denotes the superlattice potential for conduction and valence states, and F is used for the homogeneous external field. In order to calculate the eigenstates, we solve Eq. (2) first for the case $F=0$ by means of a plane-wave expansion. From the resulting Bloch functions, the exact Wannier functions of the superlattice are obtained as usual. In a second step these functions are used to expand the states $\phi_n^{c,v}(z)$. This way an accurate representation of the Wannier-Stark states of an infinite superlattice is obtained, without approximations in terms of single-well states. In contrast to the frequently used $\mathbf{k}$-space representation in which an on-site Coulomb interaction is assumed,[7] the Wannier-Stark representation allows for a more rigorous treatment and even more for an immediate physical classification of the various interaction contributions.

Optical and transport properties are determined by the distribution functions $f^a_{n-n'}$ and transition amplitudes $p^{ab}_{n-n'}$ which result from the one-particle Green's functions.[9] The superscripts a or b, respectively, are used here denoting either the conduction or the valence band. Owing to translational invariance, these functions depend only on the difference of Wannier-Stark indices, and we have in the present case the relations

$$f^a_{n-n'}(\mathbf{k},t) = i\hbar\langle\phi^a_n|G^<_{aa}(\mathbf{k},z,t,z',t)|\phi^a_{n'}\rangle \tag{3}$$

and

$$p^{ab}_{n-n'}(\mathbf{k},t) = i\hbar\langle\phi^a_n|G^<_{ab}(\mathbf{k},z,t,z',t)|\phi^b_{n'}\rangle, \tag{4}$$

respectively. In this mixed representation Green's functions obey the equation of motion

$$\left(i\hbar\frac{\partial}{\partial t} - \Delta_{ab}(\mathbf{k},z,z')\right)G^<_{ab}(\mathbf{k},z,t,z',t)$$

$$= -\sum_{b'}\int dz_1[\Omega_{ab'}(\mathbf{k},z,z_1,t)G^<_{b'b}(\mathbf{k},z_1,t,z',t)$$

$$- G^<_{ab'}(\mathbf{k},z,t,z_1,t)\Omega_{b'b}(\mathbf{k},z_1,z',t)] + \frac{\partial}{\partial t}G^<_{ab}\Big|_{\rm sc}. \tag{5}$$

Here, we have already anticipated a Markovian treatment of scattering processes and considered only the limit of equal times.

The various quantities are defined as follows. The kinetic-energy contribution of bands a and b in the effective-mass approximation is given by

$$\Delta_{ab}(\mathbf{k},z,z') = \hbar^2\mathbf{k}^2/2m_a + h^a(z) - \hbar^2\mathbf{k}^2/2m_b - h^b(z'). \tag{6}$$

For $a\neq b$, the generalized Rabi frequency is written as

$$\Omega_{ab}(\mathbf{k},z,z',t) = \mathbf{d}_{ab}\mathbf{E}(t)\,\delta(z-z') + \Sigma^{\rm HF}_{ab}(\mathbf{k},z,z',t), \tag{7}$$

with the optical field $\mathbf{E}$, the interband dipole matrix elements $\mathbf{d}_{ab}$, and the static Hartree-Fock (HF) renormalization given by

$$\Sigma^{\rm HF}_{ab}(\mathbf{k},z,t,z',t) = \sum_{\mathbf{k}'} v(\mathbf{k}-\mathbf{k}',z-z') \times[i\hbar G^<_{ab}(\mathbf{k}',z,t,z',t) - \delta_{ab}\delta_{av}\delta(z-z')], \tag{8}$$

where $v(\mathbf{k},z) = 2\pi e^2\exp(-|\mathbf{k}||z|)/(A\varepsilon|\mathbf{k}|)$ is the bare Coulomb interaction. Since the interband dipole matrix elements vanish for $a=b$, Eq. (7) [or Eq. (8)] represents the exchange self-energy in this case.

The scattering contributions in the equation of motion (5) are given by

$$\frac{\partial}{\partial t}G^<_{ab}(\mathbf{k},12)\Big|_{\rm sc} = -\sum_{b'}\int d3(\{[\Sigma^<_{ab'}(\mathbf{k},13)G^>_{b'a}(\mathbf{k},32) - G^<_{ab'}(\mathbf{k},13)\Sigma^>_{b'a}(\mathbf{k},32)] \times\theta(t_1-t_3)\} - \{<\rightleftharpoons>\}), \tag{9}$$

with the abbreviation $1=\{z_1,t_1\}$, and $t_1=t_2$. Assuming a binary collision approximation, we have for the self-energies

$$\Sigma^{\lessgtr}_{ab}(\mathbf{k},z,t,z',t')$$

$$= \hbar^2\sum_{a'b'\mathbf{k}'\mathbf{q}}\int dz_1dz_2w(\mathbf{q},z-z_1)[G^{\lessgtr}_{ab}(\mathbf{k}-\mathbf{q},z,t,z',t') \times G^{\gtrless}_{a'b'}(\mathbf{k}'-\mathbf{q},z_2,t',z_1,t)G^{\lessgtr}_{b'a'}(\mathbf{k}',z_1,t,z_2,t') \times w(\mathbf{q},z_2-z') - G^{\lessgtr}_{aa'}(\mathbf{k}-\mathbf{q},z,t,z_2,t') \times G^{\gtrless}_{a'b'}(\mathbf{k}'-\mathbf{q},z_2,t',z_1,t)G^{\lessgtr}_{b'b}(\mathbf{k}',z_1,t,z',t') \times w(\mathbf{k}-\mathbf{k}',z_2-z')], \tag{10}$$

with $w(\mathbf{k},z)$ being the statically screened Coulomb interaction. The spatial dependence is treated by means of the expansion

$$G^{\lessgtr}_{ab}(\mathbf{k},z,t,z',t') = \sum_{nn'} g^{\lessgtr ab}_{n-n'}(\mathbf{k},t,t')\phi^a_n(z)\phi^{b*}_{n'}(z') \tag{11}$$

into the Wannier-Stark solutions of Eq. (2). Finally, we obtain the Markovian version of the kinetic equations by reducing the two-time propagators to single-time functions. This is accomplished by the ansatz

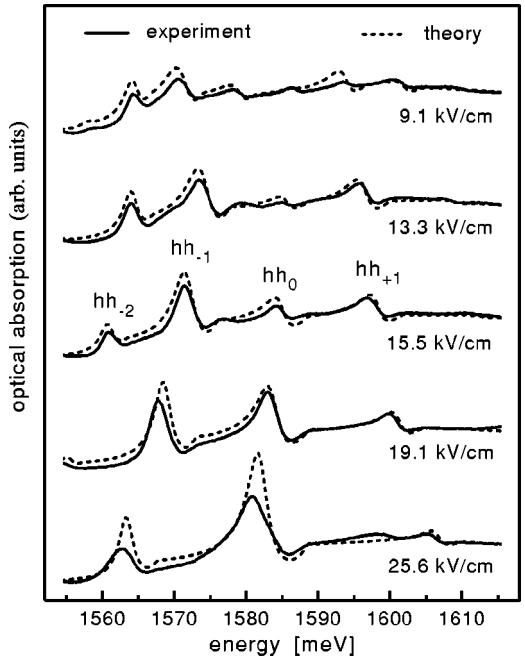

FIG. 1. Experimental and theoretical absorption spectra of a biased 67/17-Å superlattice. Note the typical Fano line shape of all transitions and the decreased broadening for growing field and falling ladder index, respectively.

$$g^{\lessgtr ab}_{n-n'}(\mathbf{k},t,t') = S^a_n(\mathbf{k},t-t')g^{\lessgtr ab}_{n-n'}(\mathbf{k},t,t) + S^b_{n'}(\mathbf{k},t'-t) \times g^{\lessgtr ab}_{n-n'}(\mathbf{k},t',t'),$$

$$\text{with} \quad S^a_n(\mathbf{k},t-t') = \theta(t-t')\exp[-iE^a_n(\mathbf{k},t-t')]. \tag{12}$$

This way the kinetic equations are transformed into a form which is solved numerically. The Hartree-Fock contributions are the same as those derived earlier within the density-matrix theory.[10] Basically, our theory contains no adjustable parameters (apart from an overall normalization factor). Thus, a direct comparison of the theory with both linear and nonlinear experimental data provides direct identification of the physical mechanisms governing the dynamics in semiconductor superlattices.

The first severe touchstone of our approach is the absorption spectra of the biased superlattice. Figure 1 shows a number of calculated and measured absorption spectra for several fields, with the absolute magnitude being the only free parameter. The potential drop over one superlattice period varies from 7.6 to 21.5 meV in the considered range. This is well above an estimated exciton binding energy of 6 meV, hence ensuring a degeneracy of a Wannier-Stark exciton with the continuum of the next lower subband. The Wannier-Stark excitons are labeled hh_0 for the heavy-hole exciton with electron and hole centered in the same well, or $hh_{\pm n}$ for the electron centered n wells to the energetically raised or lowered side, respectively. As shown in the figure, all peaks exhibit the typical asymmetric Fano line shape as soon as they are clearly resolved from the continuum. The broadening of the Fano line shape is reduced with growing fields[8] in accordance with a reduced Fano coupling of the Wannier-Stark subbands. Apart from some minor deviations (due to the neglected light holes in the model), the theory reproduces excellently the linear response.

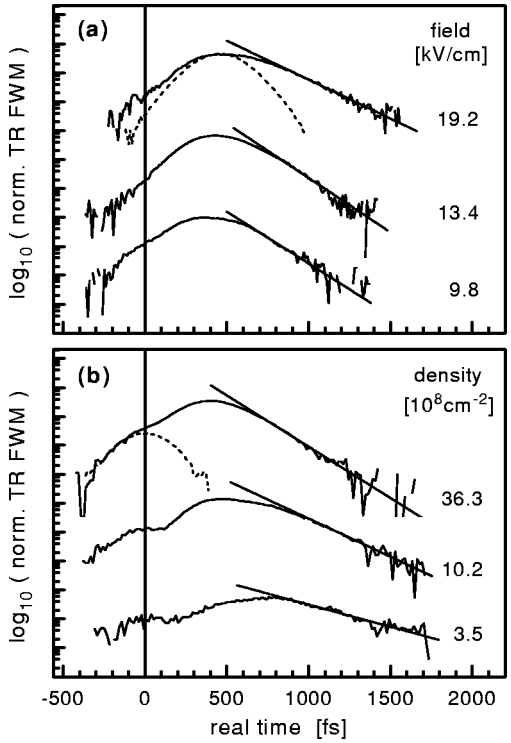

FIG. 2. Experimental TR FWM signals of the hh_{-1} transition for a pump-probe delay $T_{12}=0$ fs. (a) Tuning of the bias field at an excitation density of 1.62×10^9 cm^{-2} and (b) variation of the excitation density at a fixed field of 15.0 kV/cm. The shoulder at $t=0$ is upconverted stray light of the probe pulse (dashed line: autocorrelation of laser pulse).

The pronounced Fano broadening should also be reflected in the polarization dynamics, which is studied by TR FWM. We use 250-fs pulses of a Ti:sapphire laser (7-meV full width at half maximum) tuned 1 meV below the exciton resonance. Thus, we avoid scattering with free-continuum states of the same subband to a great extent.[11] The experiments were carried out in transmission geometry at 15 K. The time scale of the polarization dynamics starts with the arrival of the FWM probe pulse which physically triggers the signal emission. A pump-probe delay $T_{12}=0$ fs is used for all of the presented data.

The TR FWM traces obtained [see Fig. 2(a)] exhibit an exponential decay over two decades well resolved above the autocorrelation limit. The maxima of the traces are shifted in the order of 500 fs (and even more for lower densities) with respect to the FWM probe pulse. This delay is expected as consequence of the Coulomb interaction[9] and scales with the dephasing time.

The increase of the linewidth obtained from the linear spectra, however, does not simply transform into a reduced decay time of the TR FWM signal. In contrast, the decay of the *linear* polarization reflects directly the Fano broadening, and is compared in Fig. 3 with the experimental TR FWM decay rates for various fields at an excitation density of

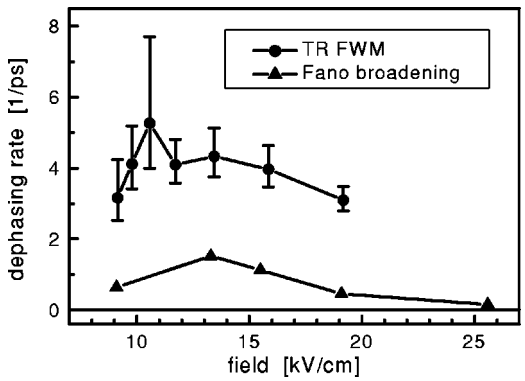

FIG. 3. Dephasing rate of the hh_{-1} transition in a 67/17-Å superlattice vs bias field at an excitation density of 1.62×10^{9} cm^{-2}. Comparison of the TR FWM data (circles) with the linear polarization decay (triangles).

1.62×10^{9} cm^{-2}. As is already apparent from the absorption spectra, the first-order polarization decay undergoes a strong relative variation. We find a change from 1.5 ps^{-1} at 13.3 kV/cm to nearly zero at higher fields. This is exactly the behavior expected for decreasing Fano coupling strength with growing ladder separation and is completely different from the results of the third-order experiments. Although there is a tendency of decreasing dephasing rates with increasing fields, the decay of the TR FWM signal occurs on a much faster scale. The origin of this effect is the interference of the various polarizations at the same transition energy, which contribute to the FWM signal.

In order to obtain a more detailed physical insight, it is instructive to consider the various Wannier-Stark subband couplings and interaction contributions, which occur in the kinetic equations. The first one is due to the sum over the various Rabi frequencies $\Omega_m(\mathbf{k})=\mathbf{d}_m^{cv}\mathbf{E}+\Sigma_{n'\mathbf{k}'}v_{mn'}^{cv}(\mathbf{k}-\mathbf{k}')p_{n'}^{cv}(\mathbf{k}')$ in the source of Eq. (5) using Eq. (7). This sum gives rise to the Fano coupling in the linear spectra. Second, as a pendant of this coupling, we obtain contributions of the form $\Sigma_m p_{n+m}^{cv*}(\mathbf{k})\Omega_m(\mathbf{k})$ in the source of the one-particle distributions, which lead to pronounced interference effects in the density modulation and thus in the FWM signals, as is demonstrated in Fig. 4. These contributions are present even at low densities and influence the decay of the diffracted signal independent of excitation-induced dephasing.

The left-hand side shows the results of a full calculation for different fields at $n=1.73\times10^{9}$ cm^{-2}. Both the decay time and the delay of the signal are in good agreement with the experimental findings. The fast initial decay of the TR FWM signal results from the interference of the occupation of different Wannier-Stark subbands. For larger times the decay rate approaches asymptotically a value, which is determined by the Fano broadening and the density-induced contributions. This appears to be similar to earlier observations[14,12,13] where the *time-integrated* FWM signal decays faster than the dephasing time of the exciton due to coherent exciton-continuum scattering. However, these authors obtain a long decay time in the *time-resolved* four-wave mixing coinciding with the dephasing time, in contrast to the result of this study.

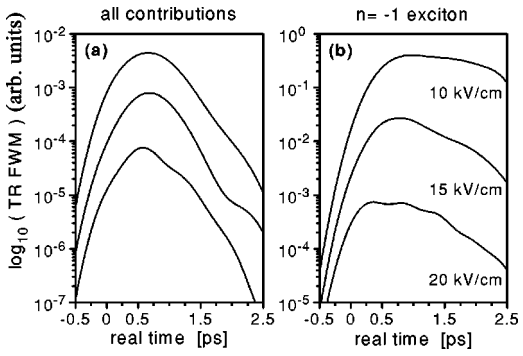

FIG. 4. Calculated TR FWM signals at 10, 15, and 20 kV/cm (bottom to top) and at a density of 1.73×10^{9} cm^{-2}. (a) Results of a full calculation; for clarity the middle and the lower signal are reduced by a factor of 10 and 100, respectively. (b) Results of a calculation, in which only the $n=-1$ exciton is taken into account; for details see text.

The fast decay of the TR FWM signal can in fact be explained by a complex coupling of the various Wannier-Stark subbands. If the excitation of the subbands is restricted to the dominant Wannier-Stark exciton, we obtain a behavior (at the same excitation density) completely different to the case before. Taking only the $p_{n=-1}^{cv}$, the $f_{n=0}^{c}$, and the $f_{n=0}^{v}$ contributions into account, we find indeed a field dependence of the decay time, which is very similar to the dependence, expected from the Fano broadening of the linear spectra. This is demonstrated on the right-hand side of Fig. 4. But now, the decay times themselves and the field dependence of the signal magnitudes are completely wrong compared with experiment. All calculations are done at a density similar to the relatively weak excitation during the experiment, and include excitation-induced scattering. Although Fig. 2(b) shows a density dependence of the decay time in experiment, an extrapolation to the low-density limit cannot resolve the fact that there is obviously no agreement of decay time and signal delay between experiment and theory. Our theoretical investigations thus show that the initial decay of the TR FWM signal is determined by the interference resulting from the simultaneous occupation of different Wannier-Stark subbands and does not reflect the Fano linewidth found in linear absorption.

With increasing density, the scattering contributions in Eq. (9) become perceptible which are responsible for excitation-induced dephasing and carrier relaxation. Again we have to distinguish between various types of interactions. The one-particle distribution $f_{n=0}$ describes the sum over the occupation of all Wannier-Stark levels. The leading relaxation channel is the scattering with other $f_{n=0}$ contributions and is essentially the same as in a single quantum well. On the other hand, the coupling to the intraminiband transition amplitudes $f_{n\neq0}$, which are responsible for Bloch oscillations and terahertz emission, has the tendency to maintain coherence and to increase the dephasing times of interband transitions. Thus the decay of the interband polarization is slower than the relaxation of the occupation or the decay of the occupation modulation. Physically, the rapid decay of the occupation modulation is an immediate result of the strong

inhomogeneity, owing to the superlattice potential, and is missing in homogeneous systems. As a further consequence, scattering with coherent carriers, for which intrasubband transitions are still present, is less effective than with incoherent ones. This was found experimentally, too.[15] The mechanism of this interplay of coherent and incoherent scattering contributions is basically the same as that found for the interminiband transitions in quantum cascade structures.[16,17]

An immediate consequence of this interplay is the density dependence of the TR FWM signals. Whereas the linear dependence of the dephasing rate is less surprising [accompanied by a shift of the maximum to smaller times; see Fig. 2(b)], we obtain an extremely unusual linear dependence of the FWM intensity (Fig. 5). This is in striking contrast to simple perturbational results, where the FWM intensity increases with the third power of the excitation density. The effect originates in the compensation of the increase of the occupation modulation by its fast decay on a time scale of a few 100 fs. The linear dependence is observed over the full varied range though only moderate excitation densities are applied. Bleaching of the states does not occur at this level.

In conclusion, we have shown the huge impact of intraminiband coupling on the carrier dynamics in superlattices. In the linear regime, coupling of excited excitons to the degenerate continua of other Wannier-Stark subbands results in a bias-field-dependent Fano broadening of the linewidth which is also reflected in the *linear* polarization decay rate. However, we find a substantial difference between the Wannier-Stark linewidth and the *nonlinear* polarization decay. The polarization interference resulting from the simultaneous occupation of different Wannier-Stark subbands leads to a fast initial decay of the time-resolved FWM signal. For larger times, the decay rate is reduced and is determined by Fano broadening and density-induced scattering. Moreover, we observe a highly unusual linear increase of the TR FWM intensity with density. The signal increase caused by a growing occupation modulation is directly compensated by a fast decay of this modulation due to coupling of the subbands. The experimental findings can be quantitatively explained by means of numerical evaluation of the kinetic equations obtained within the Born-Markov approximation.

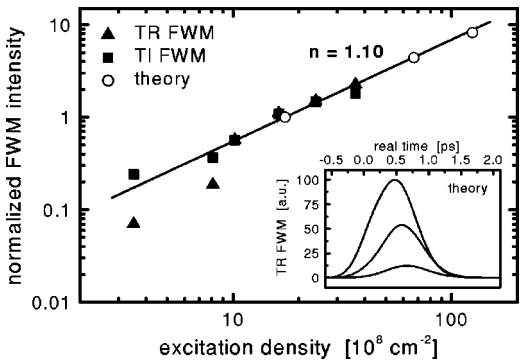

FIG. 5. FWM signal intensity vs excitation density obtained from the hh_{-1} transition (67/17-Å superlattice, 15.0 kV/cm, TR FWM at $T_{12}=0$ fs). The line is added for comparison of the slope. The inset shows the calculated TR FWM signals at densities of $(1.73/6.72/12.5)\times 10^9$ cm^{-2} and at the same field.

[1] U. Fano, Phys. Rev. **124**, 1866 (1961); U. Fano and J.W. Cooper, Phys. Rev. **137**, A1364 (1965).
[2] M. Glass-Maujean, H. Frohlich, and J.A. Beswick, Phys. Rev. Lett. **61**, 157 (1988).
[3] A.A. Clerk, X. Waintal, and P.W. Brouwer, Phys. Rev. Lett. **86**, 4636 (2000); J. Göres, D. Goldhaber-Gordon, S. Heemeyer, M.A. Kastner, H. Shtrikman, D. Mahalu, and U. Meirav, Phys. Rev. B **62**, 2188 (2000).
[4] C. Goffaux, J. Sánchez-Dehesa, A. Levy Yeyati, Ph. Lambin, A. Khelif, J.O. Vasseur, and B. Djafari-Rouhani, Phys. Rev. Lett. **88**, 225502 (2002).
[5] See, e.g., D.Y. Oberli, G. Böhm, G. Weimann, and J.A. Brum, Phys. Rev. B **49**, 5757 (1994); U. Siegner, M.-A. Mycek, S. Glutsch, and D.S. Chemla, Phys. Rev. Lett. **74**, 470 (1995); S. Glutsch, D.S. Chemla, and F. Bechstedt, Phys. Rev. B **51**, 16 885 (1995); B. Pal and A.S. Vengurlekar, Appl. Phys. Lett. **79**, 72 (2001); K.C. Hall, G.R. Allan, H.M. van Driel, T. Krivosheeva, and W. Pötz, Phys. Rev. B **65**, 201201 (2002).
[6] T. Meier, A. Schulze, P. Thomas, H. Vaupel, and K. Maschke, Phys. Rev. B **51**, 13 977 (1995).
[7] R.-B. Liu and B.-F. Zhu, Phys. Rev. B **59**, 5759 (1999).
[8] C.P. Holfeld, F. Löser, M. Sudžius, K. Leo, D.M. Whittaker, and K. Köhler, Phys. Rev. Lett. **81**, 874 (1998).
[9] W. Schäfer and M. Wegener, *Semiconductor Optics and Transport Phenomena* (Springer-Verlag, Berlin, 2002), and references therein.
[10] M.M. Dignam, Phys. Rev. B **59**, 5770 (1999).
[11] We have also done a series of TR FWM measurements with a systematic variation of the laser detuning relative to the resonance. There is only a weak dependence of dephasing time and signal shape, indicating a minor influence of optical coupling within one subband in respect to Fano coupling.
[12] M.U. Wehner, D. Steinbach, and M. Wegener, Phys. Rev. B **54**, R5211 (1996).
[13] D. Birkedal, V.G. Lyssenko, J.M. Hvam, and K. El Sayed, Phys. Rev. B **54**, 14 250 (1996).
[14] K. El Sayed, D. Birkedal, V.G. Lyssenko, and J.M. Hvam, Phys. Rev. B **55**, 2456 (1997).
[15] F. Wolter, R. Martini, S. Tolk, P. Haring Bolivar, H. Kurz, R. Hey, and H.T. Grahn, Superlattices Microstruct. **26**, 93 (1999).
[16] F. Eickemeyer, K. Reimann, M. Woerner, T. Elsaesser, S. Barbieri, C. Sirtori, G. Strasser, T. Müller, R. Bratschitsch, and K. Unterrainer, Phys. Rev. Lett. **89**, 047402 (2002).
[17] R.C. Iotti and F. Rossi, Phys. Rev. Lett. **87**, 146603 (2001).